TOMSK POLYTECHNIC UNIVERSITY

Available online at www.sciencedirect.com

ScienceDirect

Resource-Efficient Technologies 3 (2017) 29–36

www.elsevier.com/locate/reffit

Research paper

Waste walnut shell valorization to iron loaded biochar and its application to arsenic removal

Xinhui Duan [a,b,c,*], Chengcheng Zhang [a,b,c], C. Srinivasakannan [d], Xin Wang [e]

[a] Institute of Power Source and Ecomaterials Science, Hebei University of Technology, Tianjin 300130, China

[b] Key Laboratory of Special Functional Materials for Ecological Environment and Information, Hebei University of Technology, Ministry of Education, Tianjin 300130, China

[c] Key Laboratory for New Type of Functional Materials in Hebei Province, Hebei University of Technology, Tianjin 300130, China

[d] Chemical Engineering Program, The Petroleum Institute, P.O. Box 2533, Abu Dhabi, United Arab Emirates

[e] School of Environmental Science and Engineering, Hebei University of Science and Technology, Shijiazhuang, Hebei 050018, China

Received 5 September 2016; received in revised form 16 November 2016; accepted 1 January 2017

Available online 2 February 2017

Abstract

Iron loaded biochar (ILB) was prepared from waste walnut shell by microwave pyrolysis and its application for arsenic removal was attempted. The ILB was characterized using X-ray diffraction, scanning electron microscopy and BET Surface area analyzer. The adsorption isotherm of As (V) in ILB covering a temperature range of 25 to 45 °C, as well as the kinetics of adsorption at 25 °C were experimentally generated. The adsorption isotherms were modeled using Langmuir and Freundlich isotherm models, while the kinetics of adsorption was modeled using the pseudo-first-order, pseudo-second-order kinetic models, and intra particle diffusion model. The ILB had a surface area of 418 m^2/g with iron present in the form of hematite (Fe_2O_3) and magnetite (Fe_3O_4). The arsenic adsorption isotherm matches well with Langmuir isotherm model with a monolayer adsorption capacity of 1.91 mg/g at 25 °C. The adsorption capacity of As (V) well compares with other porous adsorbents widely reported in literature, supporting its application as a cost effective adsorbent.

Keywords: Biochar; Water treatment; Adsorbent; Kinetics; Thermodynamic

1. Introduction

Presence of arsenic in natural water sources has been a serious concern worldwide. In many parts of the world, the underground water is contaminated with arsenic. The arsenic contaminated tube-wells are the only viable source for drinking water in most of the underdeveloped countries, even today. In most of these cases, the groundwater is potable, excepting the presence of unacceptable level of arsenic. Arsenic is a carcinogen and its ingestion may deleteriously affect the gastrointestinal tract, cardiac, vascular system and central nervous system. Due to its high toxic effect on human health, the USEPA has lowered the maximum contaminant level in drinking water to 10 μg/l. Arsenic contamination of the ground water occurs through natural processes such as weathering of arsenic containing minerals, anthropogenic activities such as uncontrolled industrial discharge from mining and metallurgical industries, and application of organo-arsenical pesticides [1–4].

Literature survey reveals that there are number of approaches for arsenic removal from water. The most commonly used treatment techniques for arsenic removal include coagulation with iron and aluminum salts; ion-exchange, reverse osmosis and electro-dialysis; adsorption onto activated alumina/carbon, activated bauxite, clay minerals and iron oxides, et al. [5–7]. The treatment methods such as ion exchange and reverse osmosis are expensive, which hinder the further application in large scale. The chemical precipitation with lime/ferric salt reported to be effective, but yields large quantities of solid sludge, which demands further treatment. Due to simplicity of the process as well as being re-generable, the adsorption technology has been widely used to remove arsenic.

* Corresponding author. Institute of Power Source and Ecomaterials Science, Hebei University of Technology, Tianjin 300130, China. Tel.: +86 60204850.

E-mail address: dxh1191984@aliyun.com (X. Duan).

http://dx.doi.org/10.1016/j.reffit.2017.01.001

Biochar is a black carbon prepared through thermal or hydrothermal conversion of biomass, which is highly recommended for soil amendment due to its ability to reduce greenhouse gases as well as to enhance soil fertility by improving moisture and nutrients retention [8]. Its application for utilization as adsorbent for removal of containments such as heavy metals and organic compounds in water and soil has also been reported [9]. Large varieties of renewables such as agriculture waste, forestry and animal husbandry are utilized for production of biochar at low cost. With certain modifications, either physical or chemical treatment the biochar utility can be enhanced, rendering it suitable for different environmental application.

Pyrolysis is a thermochemical method in the absence of oxygen to convert biomass into biochar, usually refers to conventional heating for long duration that virtually increases cost of biochar produced. Microwave assisted pyrolysis is being increasingly utilized to produce biochar as it is energy efficient and is a clean method of heating in addition to producing biochar that possesses higher surface area than conventional heating [10]. Iron oxide coated over variety of porous precursors such as alumina, activated carbon, cloth fibers, aerogels, fly ash, membranes is of recent research interest for removal of As (V). As compared to popular iron coated porous adsorbents, ILBs are cost effective alternatives [11]. Pyrolysis of iron salt solution impregnated biomass to prepare ILB is a popular method as it is a single stage process.

Walnut in China is a cash crop, processing of which was reported to produce more than 0.5 million ton of walnut shell as byproduct per year. Common way of utilization of this carbon rich waste is to use it as fuel through combustion, which causes serious environmental problems. Toward this, the present study attempts to prepare a microwave pyrolyzed ILB from walnut shell and assess its potential as a low cost adsorbent for arsenic removal. The adsorption isotherms as well as the kinetics of adsorption data are generated and appropriately modeled.

2. Experimental

2.1. Materials

The waste walnut shell collected from local market washed thoroughly using deionized water to remove impurities, crushed and sieved into size fractions about 2 mm, dried at 105 °C overnight and stored in desiccators for later utilization, its proximate analysis along with the ultimate analysis is reported in Table 1.

All chemicals used in this study, including ferric chloride ($FeCl_3/6H_2O$), sodium arsenate ($Na_2HAsO_4/7H_2O$) were of analytical grade. Synthetic arsenate contaminated solution was prepared with sodium arsenate in deionized water with different initial concentrations.

2.2. Preparation of ILB

The microwave assisted pyrolysis is carried out in a microwave tubular furnace with microwave frequency of 2.45 GHz and maximum microwave output power of 1200 W, the schematic diagram of the microwave heating system can be seen elsewhere [12]. First an iron contained solution was prepared by dissolving 30 g $FeCl_3$ in 70 ml deionized (DI) water, and the dry walnut shell was impregnated with the solution for 4 h, then the solid was separated and dried at 105 °C for 2 h. The pretreated sample was loaded in a quartz reactor and pyrolyzed in the microwave tubular furnace at microwave power of 800 W for 20 min, in N_2 atmosphere. The samples were repeatedly rinsed with DM water, dried at 100 °C, and stored in sealed container for further experimentation.

2.3. Adsorption of arsenic

Batch adsorption experiments are performed in a set of Erlenmeyer flasks (250 ml), each containing 100 ml of different initial concentrations of As(V) (0.1–5 mg/L), together with 0.1 g of ILB, the pH is adjusted to 7 by addition of HCl and NaOH solution (0.1 mol/L). A gas bath thermostatic oscillator utilized to maintain the desired temperature for desired duration of adsorption. The concentrations of As(V) in the supernatant solutions are measured by an Atomic Absorption Spectrophotometer (ZA2000 Hitachi, Japan), before and after the adsorption process.

The adsorbed amount of As(V) at equilibrium, q_e (mg/g), is calculated by the following equation:

$$q_e = \frac{(C_0 - C_e)\,V}{W} \tag{1}$$

where C_0 and C_e are the initial and equilibrium As(V) concentrations(mg/L), respectively. V is the volume of solution (L) and W is the dry weight of the added adsorbent (g).

The procedure for estimation of adsorption kinetics of As(V) is basically identical to that of equilibrium tests, except for the fact that the liquid samples were taken at intervals of time, with the zero time corresponding to the time that the adsorbent is charged into the dye solution. The total volume of the liquid samples withdrawn is less than 5% of the total volume of the solution. The amount of adsorption by adsorbent at time t, q_t (mg/g), is calculated by the following equation:

$$q_t = \frac{(C_0 - C_t)\,V}{W} \tag{2}$$

Table 1
Proximate and ultimate analysis of walnut shell.

Sample	Proximate analysis (Wt. %)				Elemental analysis (Wt. %)			
	Fixed carbon	Volatiles	Ash	Moisture	C	H	O	N
Walnut shell	22.07	76.98	0.67	13.60	46.80	3.41	43.11	0.28

where C_0 and C_t are the liquid-phase concentrations at an initial and pre-determined time t (mg/L), respectively, V is the volume of solution (L) and W is the dry weight of the adsorbent (g) added.

2.4. Characterization of the ILB

The microstructures of the ILB analyzed by the scanning electron microscope (SEM-EDS, Philips XL30ESEM-TMP). The BET surface area and average pore size distribution were estimated using the surface area analyzer, Autosorb 1-C made by Quantachrome Instruments, USA. The iron types in the biochar were identified by X-ray diffraction (XRD) analysis through a Bruker D8 Discover diffractometer in Bragg–Brentano geometry, using Cu K_α radiation with a wavelength of 1.5417 nm. The powdered samples of adsorbent are scanned from 5° to 85°, using a step size of 0.02° and a run time of 1 s/step.

The acid extraction method [13] was selected to evaluate the amount of iron loaded in biochar. One hundred milligrams of the biochar is added into a 100 ml Erlenmeyer flask containing 30 ml HCl (1:1) solution and shaken for 10 h, then the Erlenmeyer flask was placed in a water bath at 70–80 °C for 4 h, the biochar is separated from the solution by filtration. The concentration of iron in the filtrate was examined using the phenanthroline method with a spectrophotometer (UV2550, Shimadzu, Japan).

3. Result and discussion

3.1. Characterization of the ILB

The XRD analysis identifies the iron species loaded in the biochar. The XRD spectra shown in Fig. 1 match well with the crystalline iron species of hematite (Fe_2O_3) and magnetite (Fe_3O_4). Zhang et al. [10] have reported iron content in the form of maghemite (γ-Fe_2O_3) in the cotton wood biochar pyrolyzed at temperature of 600 °C by conventional heating. While Liu and Zhang [14] reported a pure magnetite (Fe_3O_4) in the sawdust based biochar pyrolyzed at 600 °C by conventional heating. The variation in the form of iron in the biochar could possibly be due to the variation in the content of the raw material as well as the processing conditions. The iron content in the ILB prepared in the present work was 19.05%, which was estimated using acid extraction method.

The pore structure of the ILB was characterized using nitrogen adsorption at 77 K with an accelerated surface area and porosimetry system (Autosorb-1-C, Quantachrome). Prior to gas adsorption measurements, the sample was degassed at 300 °C in a vacuum condition for a period of at least 16 h. Nitrogen adsorption isotherm was measured over a relative pressure (P/P_0) range of approximately 10^{-7} to 1. The BET surface area was calculated from the isotherms by using the Brunauer–Emmett–Teller (BET) equation. The cross-sectional area for nitrogen molecule was assumed to be 0.162 nm^2. The

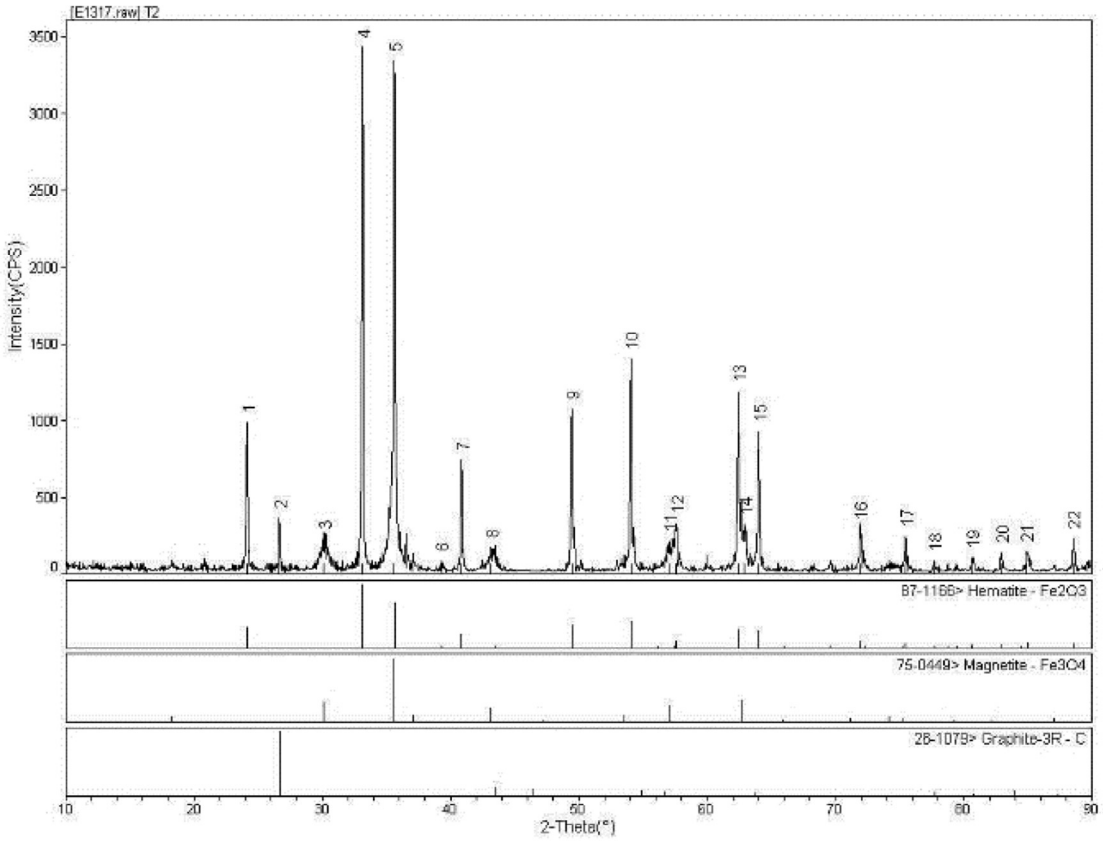

Fig. 1. X-ray diffraction spectra of iron loaded adsorbent.

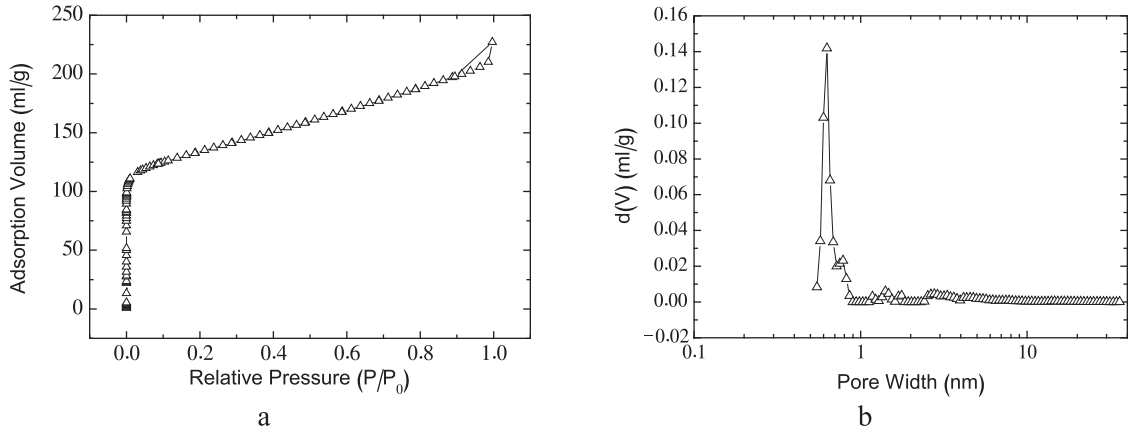

Fig. 2. Nitrogen adsorption isotherms of ILB (a) and Pore size distribution of ILB (b).

micropore size distribution was estimated using the Non-local Density Functional Theory (NLDFT) model. The total volume was estimated by converting the amount of N_2 gas adsorbed at a relative pressure of 0.95 to equivalent liquid volume of the adsorbate (N_2).

Fig. 2a shows the nitrogen adsorption isotherm of the ILB estimated using the Autosorb instrument. As can be seen in the figure, it exhibits a sharp increase in the volume adsorbed at low relative pressure, which indicates the process of micro pore filling. This type of isotherms is characteristic of type IV, which indicates presence of both micro as well as mesoporous. Fig. 2b shows the pore size distribution of the ILB, with sharp peaks in the range of 0.5 to 0.7 nm, indicating proportion of micropores. The BET surface area and total pore volume of the ILB is estimated to be 418 m^2/g and 0.35 ml/g, respectively. Biochar prepared through conventional pyrolysis methods was known to be less porous with surface area not more than 100 m^2/g. The high surface area of ILB attributed to activation induced by the $FeCl_3$ that additionally contributed to the formation of pores. Mubarak et al [15] have reported better pore structure of the biochar from palm oil empty fruit bunch pyrolyzed in presence of $FeCl_3$.

Fig. 3 shows the microscopic structure of the ILB, along with the EDS analysis. It is evident that the surface of the biochar evenly covered by globular particles of different size. The EDX analysis reveals that the composition of white particles mainly corresponds to Fe and oxygen elements, which is in good agreement with the XRD analysis.

3.2. Batch adsorption experiments of As(V)

3.2.1. Effect of contact time and As(V) concentration on adsorption

Fig. 4 shows the adsorption capacity of ILB at different initial As(V) concentrations and contact time at 298 K. As can be seen, the adsorption capacity increases with increase of initial concentration of As(V) and contact time. The increase in equilibrium adsorption capacity with increase in the initial concentration of the As(V) solution is well understood from the

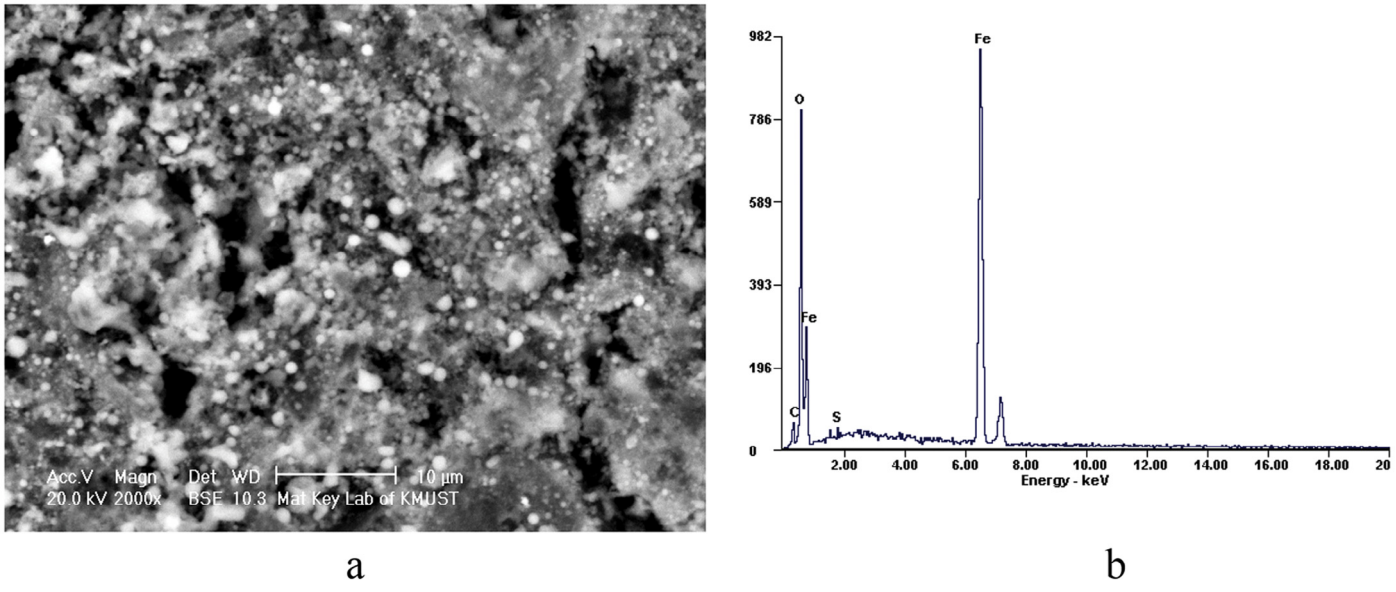

Fig. 3. SEM images and EDX analysis of the ILB.

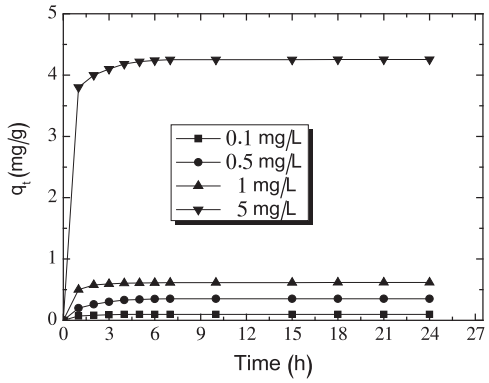

Fig. 4. The variation of adsorption capacity with adsorption time at various arsenic concentrations at 298K (pH = 7, adsorbent amount of 0.1g).

basic concepts of the equilibrium adsorption isotherms. It is clear from the figure that majority of As(V) is adsorbed within contact time of 5 to 7 hours while it attained equilibrium after 10 hours. The higher rate of removal might be due to the sorbent sites being vacant initially in addition to high solute concentration gradient. Mondal et al. [6] also reported that the increase of initial concentration would increase the ratio of the number of adsorbate moiety to the available active sites of adsorbent.

3.2.2. Adsorption isotherms

The adsorption isotherms were generated following the procedure as stated in section 2.3, in accordance with the literature by varying the initial concentration of As(V) at three different temperatures of 298, 303 and 308 K [16]. The experimental data plotted in accordance with the popular Langmuir and Freundlich adsorption isotherms is shown in Fig. 5 for the ILB. The estimated model parameters are presented in Table 2. Based on the R^2 reported in Table 2, the adsorption equilibrium data match better with the Langmuir isotherm model than the Freundlich isotherm model. The adsorption capacity decreased as adsorption temperature increased. The ILB consisted of nearly 19% iron, the active form of which would bind with As (V) provided availability of sufficient activation energy for the reaction. On the other-hand, the proportion of pores in absence

Table 2
Langmuir and Freundlich isotherm model parameters and correlation coefficients for the adsorption of arsenic by iron loaded biochar.

Isotherms	Parameters	Temperature (K)		
		298	308	318
Langumir	Q_0 (mg/g)	1.91	1.24	0.92
	a_L (L/mg)	3.45	3.42	2.73
	R^2	0.98	0.99	1
Freundlich	1/n	0.88	0.90	0.99
	K_F (mg/g(L/mg)$^{1/n}$)	3.13	2.51	2.15
	R^2	0.96	0.98	0.99

of active iron content is expected to promote physisorption. The magnitude of these two competing phenomena governs either an increase or decrease in the adsorption capacity with temperature. An increased proportion of physisorption would contribute to a decrease in adsorption capacity with an increase in temperature while an increased proportion of chemisorption in general would contribute to an increase in the adsorption capacity. The decrease in equilibrium adsorption with increase in temperature clearly indicates a significant proportion of Phyisorption along with Chemisorption. Additionally, at high temperatures increased rate of reaction contributes to the rapid formation of precipitates on the surface of the carbon, reducing the access of As(V) for the active sites inside the porous structure, contributing to a decrease in the adsorption capacity with increase in temperature. Similar observations are reported in the literature [17,18].

The equilibrium constants a_L of the Langmuir model decrease as adsorption temperature increases. The parameter a_L in Langmuir model reflects the strength of binding energy between the adsorbate and the adsorbent or the affinity of the adsorbent for the adsorbate. A higher a_L reflects stronger adsorption capacity of the adsorbent to the adsorbate.

The mono layer adsorption capacity estimated based on the Langumuir isotherms model for adsorption of As(V) on the ILB is 1.91 mg/g. For the sake of comparison with other effective adsorbents reported in literature, a compilation of the maximum adsorption capacity of As(V) for different adsorbents is listed in Table 3 [19–21]. The compilation reveals the adsorption capac-

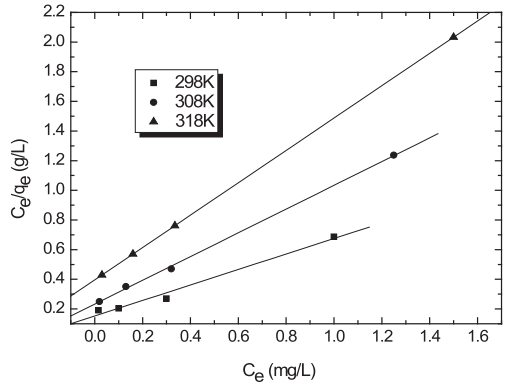

Langmuir adsorption isotherms

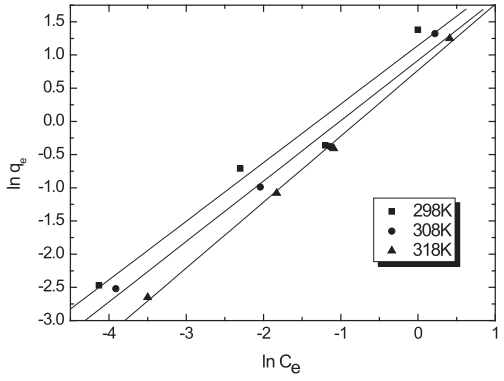

Freundlich adsorption isotherms

Fig. 5. Langmuir and Freundlich adsorption isotherm of aresnic on ILB at different temperatures.

Table 3
Comparison of As(V) adsorption capacity of various adsorbents.

Adsorbents	As(V) adsorption capacity (mg/g)	References
Biochar/ γ-Fe_2O_3 composite	3.14	Zhang et al. [10]
Granular Activated carbon-Fe	2.96	Gu et al. [16]
Fe(III)–Si binary oxide adsorbent	2.01	Zeng [19]
Fe(II)-loaded activated carbon	2.03	Tuna et al. [20]
Iron coated clay	3.12	Haque et al. [21]
Iron loaded biochar	1.91	Present work

ity of ILB is of the same order of magnitude as the best of adsorbents reported in literature. However, it should be taken into consideration that ILBs could be a cost effective replacement as compared to most of the other adsorbents. Microwave pyrolysis of $FeCl_3$ impregnated walnut shell serve to generate high surface area along with significant proportion of iron content rendering the ILBs to compete with the best of adsorbents reported in literature.

3.2.3. Adsorption thermodynamics

The thermodynamic parameters of Gibbs free energy (ΔG^0), entropy (ΔS^0) and enthalpy (ΔH^0) were calculated from experimental isotherm at different temperatures, which are listed in Table 4 for the iron loaded char. These parameters were determined using the following equation.

$$Kc = \frac{q_e}{C_e} \tag{3}$$

Where Kc is the distribution coefficient, q_e (mg/g) and C_e (mg/) are the amount of adsorbate on adsorbent phase and aqueous phase, respectively. Kc is determined from the slope of ln (q_e/C_e) against C_e at different temperatures and extrapolating to zero C_e as suggested by the method of Khan and Singh.

The standard enthalpy change of adsorption (ΔH^0) and the standard entropy change of adsorption (ΔS^0) were calculated from the slope and intercept of Van 't Hoff plot ($\ln K_C$ versus 1/T) according to Eq. (4), the standard free energy change of adsorption (ΔG^0) was determined with the same equation [22] as well.

$$\ln K_c = -\frac{\Delta G_0}{RT} = \frac{\Delta S_0}{R} - \frac{\Delta H_0}{RT} \tag{4}$$

where R is the universal gas constant and T refers to absolute temperature (K).

Table 4
Thermodynamics parameters for the adsorption of As (V) on ILB.

Sample	T (K)	ΔG (KJ/mol)	ΔH (KJ/mol)	ΔS ($J/mol^{-1}K^{-1}$)	R^2
Iron loaded biochar	298	−4.22	−37.71	−112.23	0.99
	308	−3.23			
	318	−1.97			

Table 5
Pseudo-first order and pseudo-second-order kinetic model parameters for the adsorption of arsenic by ILB at 298K.

Initial concentration (mg/L)	$q_{e,exp}$ (mg/g)	First-order kinetic model			Second-order kinetic model		
		k_1 (1/h)	$q_{e,cal}$ (mg/g)	R^2	k_2 (g/mg.h)	$q_{e,cal}$ (mg/g)	R^2
0.1	0.097	1.23	0.147	0.94	20.4	0.1	0.99
0.5	0.35	0.77	0.191	0.98	6.67	0.41	0.99
1	0.63	0.71	0.407	0.98	2.32	0.64	0.99
5	4.25	0.74	0.743	0.98	1.40	4.35	1

As can be seen in Table 4, to the iron loaded biochar, the negative ΔG^0 values for As(V) confirm the spontaneous nature of the adsorption process. Based on the enthalpy of adsorption(ΔH^0) estimated, the adsorption is exothermic in nature, substantiating the reduction in the equilibrium adsorption capacity with increase in temperature. A ΔH^0 less than 42 kJ/mol indicates the dominance of the physisorption than the chemisorption process. Chemisorption is viewed as chemical bonding while physical adsorption is viewed as a Van der Waals interaction. The negative ΔS^0 values confirm a greater order of adsorption during the adsorption of arsenate on the adsorbent, forming stable complexes between arsenate and hybrid adsorbent [23].

3.2.4. Adsorption kinetics

The adsorption kinetic experiments were performed by taking liquid samples at known intervals of time as stated in Materials and methods. The kinetics of As(V) adsorption is estimated for different initial concentrations of the dye solution ranging from 0.1 to 5 mg/L, and it is found that the rate of adsorption increase with increase in the initial concentration of the As(V) solution. The adsorption kinetics is modeled using the popular first order and second order models and the intraparticle diffusion models. As these models are widely used in the literature to model the kinetics of adsorption, the details of the model equations are not presented here and can be referred from the referred literature.

Fig. 6, plotted in accordance with the first and the second order reactions, shows the plot of adsorption kinetics of the iron loaded biochar. The model parameters and the appropriateness of the model reflecting the trend of the experimental data could be evidenced from the model parameters and R^2 values shown in Table 5. The high R^2 value close to 1 for the second-order kinetic model suggests the rate of adsorption reflects second-order kinetics.

Fig. 7 is the plot of intraparticle diffusion model plotted according to the Weber and Moris theory. If intraparticle diffusion is rate-limited then plots of adsorbate uptake q_t versus the square root of time ($t^{1/2}$) would result in a linear relationship. If the regression of qt versus $t^{1/2}$ is linear and passes through the origin, then intraparticle diffusion is the sole rate-limiting step. However, the linear plots (Fig. 7) for the iron loaded biochar at each concentration did not pass through the origin, which indicates that the intraparticle diffusion was not the only rate controlling step.

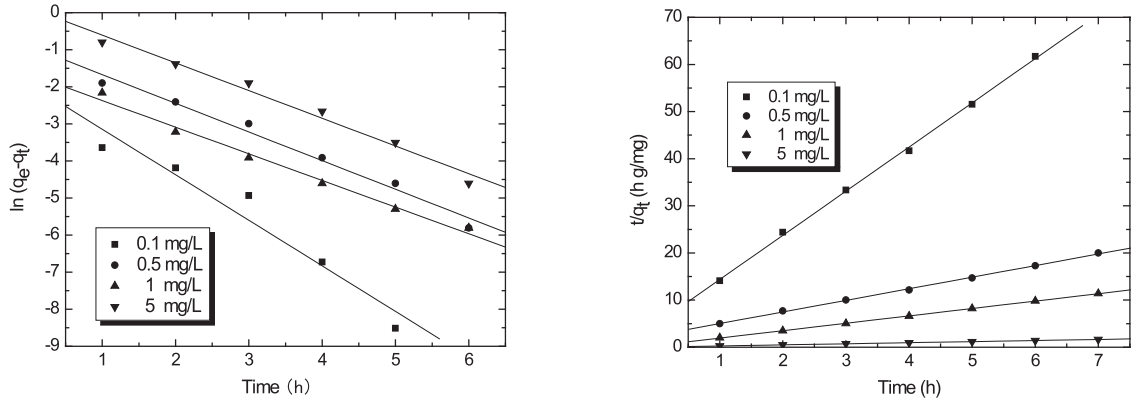

a. Pseudo-first-order kinetic b. Pseudo-second-order kinetic

Fig. 6. Pseudo-first-order and Pseudo-second-order kinetics for the adsorption of arsenic on ILB.

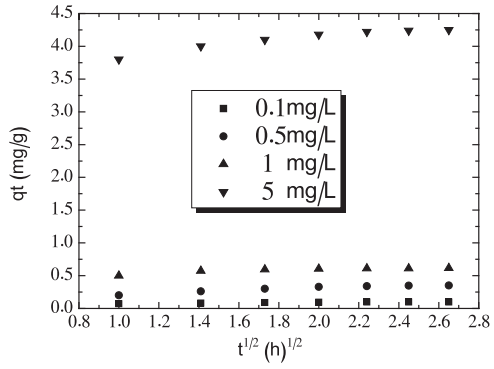

Fig. 7. Intraparticle diffusion model for the adsorption of As(V) onto ILB at 298 K.

4. Conclusions

Iron oxide coated porous materials are considered as highly promising for removal of As(V). However, they are more costly compared to ILB prepared by microwave pyrolysis, as they demand high surface area precursor and a complex impregnation process. A single step $FeCl_3$ impregnated microwave pyrolysis of walnut shell has resulted in surface area of 418 m^2/g, far superior than the biochar produced through conventional pyrolysis. The arsenic adsorption isotherm was favorably modeled using Langmuir isotherm with the maximum monolayer adsorption capacity of 1.91 mg/g at 25 °C. Kinetics of As (V) adsorption matches with pseudo-second-order kinetic model. Considering the simplicity of the process of preparing ILB, it can be an effective low cost adsorbent for arsenic removal.

Acknowledgements

The authors would like to express their gratitude to the Natural Science Foundation of Hebei Province, China (E2015202312), National High-tech R&D Program of China (2011AA03A406) and National Natural Science Foundation of China (U1402274) for financial support.

References

[1] V.C. Srivastava, M.M. Srivastava, I.D. Mall, Adsorptive removal of phenol by bagasse fly ash and activated carbon: equilibrium, kinetic and thermodynamics, Colloid Surf. A Physicochem. Eng. Asp. 272 (2006) 89–104.
[2] D. Mohan, C.U. Pittman, Arsenic removal from water/wastewater using adsorbents – a critical review, J. Hazard. Mater. 42 (2007) 1–53.
[3] M.G. Mostafa, Y.H. Chen, J.S. Jean, Kinetics and mechanism of arsenate removal by nanosized iron oxide-coated perlite, J. Hazard. Mater. 187 (2011) 89–95.
[4] Q. Chang, W. Lin, W.C. Ying, Preparation of iron-impregnated granular activated carbon for arsenic removal from drinking water, J. Hazard. Mater. 184 (2010) 515–522.
[5] H.K.M. Delowar, I. Uddin, W.H.A. Hassan, A comparative study of household groundwater arsenic removal technologies and their water quality parameters, J. Appl. Sci. 6 (2006) 2193–2200.
[6] P. Mondal, C.B. Majumder, B. Mohanty, Laboratory based approaches for arsenic remediation from contaminated water: recent developments, J. Hazard. Mater. 137 (2006) 464–479.
[7] G. Muniza, V. Fierroa, A. Celzard, Synthesis, characterization and performance in arsenic removal of iron-doped activated carbons prepared by impregnation with Fe(III) and Fe(II), J. Hazard. Mater. 165 (2009) 893–902.
[8] J. Tang, W. Zhu, R. Kookana, Characteristics of biochar and its application in remediation of contaminated soil, J. Biosci. Bioeng. 116 (2013) 653–659.
[9] L. Beesley, E. Moreno-Jimenez, J.L. Gomez-Eyles, Effects of biochar and green waste compost amendments on mobility, bio availability and toxicity of inorganic and organic contaminants in a multi-element polluted soil, Environ. Pollut. 158 (2010) 2282–2287.
[10] B.A. Mohamed, C.S. Kim, N. Ellis, Microwave-assisted catalytic pyrolysis of switchgrass for improving bio-oil and biochar properties, Bioresour. Technol. 201 (2016) 121–132.
[11] M. Zhang, B. Gao, S. Varnoosfaderani, Preparation and characterization of a novel magnetic biochar for arsenic removal, Bioresour. Technol. 130 (2013) 457–462.
[12] X.H. Duan, C.S. Kannan, Regeneration of microwave assisted spent activated carbon: Process optimization, adsorption isotherms and kinetics, Chem. Eng. Process. 53 (2012) 53–62.
[13] W.F. Chen, R. Parette, J. Zou, Arsenic removal by iron-modified activated carbon, Water Res. 41 (2007) 1851–1858.
[14] Z.G. Liu, F.S. Zhang, Arsenate removal from water using Fe_3O_4-loaded activated carbon prepared from waste biomass, Chem. Eng. J. 160 (2010) 57–62.
[15] N.M. Mubarak, A. Kundu, J.N. Sahu, Synthesis of palm oil empty fruit bunch magnetic pyrolytic char impregnating with $FeCl_3$ by microwave heating technique, Biomass Bioenergy 61 (2014) 265–275.

[16] Z.M. Gu, J. Fang, B.L. Deng, Preparation and evaluation of GAC-based iron-containing adsorbents for arsenic removal, Environ. Sci. Technol. 39 (2005) 3833–3843.

[17] P. Mondal, C. Balomajumder, B. Mohanty, A laboratory study for the treatment of arsenic, iron, and manganese bearing ground water using Fe^{3+} impregnated activated carbon: effects of shaking time, pH and temperature, J. Hazard. Mater. 144 (2007) 420–426.

[18] K. Vaca-Escobar, M. Villalobos, A.E. Ceniceros-Gomez, Natural arsenic attenuation via metal arsenate precipitation in soils contaminated with metallurgical wastes: III. Adsorption versus precipitation in clean As(V)/goethite/Pb(II)/carbonate systems, Appl. Geochem. 27 (2012) 2251–2259.

[19] L. Zeng, Arsenic adsorption from aqueous solutions on an Fe (III)–Si binary oxide adsorbent, Water Qual. Res J Can. 39 (2004) 267–275.

[20] A.O.A. Tuna, E. Ozdemir, E.B. Simsek, Removal of As(V) from aqueous solution by activated carbon-based hybrid adsorbents: impact of experimental conditions, Chem. Eng. J. 223 (2013) 116–128.

[21] N. Haque, G. Morrison, I. Cano-Aguilera, J.L. Gardea-Torresdey, Iron-modified light expanded clay aggregates for the removal of arsenic (V) from groundwater, Microchem. J. 88 (2008) 7–13.

[22] E. Ozdemir, D. Duranoglu, U. Beker, Process optimization for Cr(VI) adsorption onto activated carbons by experimental design, Chem. Eng. J. 172 (2011) 207–218.

[23] D. Pokhrel, T. Viraraghavan, Arsenic removal from aqueous solution by iron oxide-coated biomass: common ion effects and thermodynamic analysis, Sep. Sci. Technol. 43 (2008) 3545–3562.